Sn[15] surfaces, as well as on silica surface,[9] wherein the experimental curves *did* follow the strong collider curve at the same lower temperatures, indicates otherwise. The predicted magnitude of fractional surface coverage θ in such case would be only $\theta \sim 10^{-5}$ and virtually independent of temperature.

Finally the higher α_v values found in this work on metal surfaces relative to studies in other laboratories[7] may be explained by the high temperature seasoning of the surface that occurs in our work.

Acknowledgment. This work was supported by the National Science Foundation and by the Office of Naval Research.

Registry No. Cyclobutene, 822-35-5; gallium, 7440-55-3.

Methyl Isocyanide Isomerization Kinetics: Determination of Collisional Deactivation Parameters following C–H Overtone Excitation

Deanne L. Snavely,† Richard N. Zare,*

Department of Chemistry, Stanford University, Stanford, California 94305

James A. Miller, and David W. Chandler

Combustion Research Facility, Sandia National Laboratories, Livermore, California 94550
(Received: January 15, 1986; In Final Form: April 8, 1986)

The isomerization of methyl isocyanide (CH_3NC) to acetonitrile (CH_3CN) was studied by excitation of the $5\nu_{C-H}$ (726.6 nm) and $6\nu_{C-H}$ (621.4 nm) overtone states, which lie about 1 and 8 kcal/mol, respectively, above the isomerization barrier. Product yields were measured as a function of pressure and collision partner. A Stern–Volmer plot (yield^{-1} vs. pressure) shows that (1) deactivation by collision with pure CH_3NC is more rapid than with C_3H_6, SF_6, or Ar, (2) the collisional deactivation efficiencies decrease in going from C_3H_6 to SF_6 to Ar, and (3) the single-collision deactivation approximation (strong collider approximation) fails for both the $6\nu_{C-H}$ and $5\nu_{C-H}$ data. With the use of a master equation solution, assuming an "exponential down" energy-transfer function, the average energy transferred in a deactivating collision, $-\langle\Delta E\rangle_{down}$, is extracted from each data set, as well as the average energy transferred per collision, $-\langle\Delta E\rangle$. It is concluded that the isomerization yield depends markedly on the collision partner and on the average energy transferred per collision, $-\langle\Delta E\rangle$, even though the single-collision deactivation approximation might have been expected to have its greatest validity in this energy regime.

Introduction

The role of collisional deactivation in unimolecular processes continues to be controversial. Major questions remain unanswered as to (1) the magnitude of the average amount of energy transferred in a collision (or in a deactivating collision),[1] and (2) the energy dependence of $-\langle\Delta E\rangle$.[2,3] The thermal isomerization of methyl isocyanide (CH_3NC) to acetonitrile (CH_3CN), extensively investigated by Rabinovitch and co-workers,[4] has long served as a classic model for the study of unimolecular dynamics. Beginning in 1977, Reddy and Berry[5,6] used direct C–H stretch overtone excitation as a means of extending these isomerization studies beyond thermal energies and of specifying the energy content of the activated molecule with more precision. Their emphasis was on (1) the determination of the rate of unimolecular decomposition, based on the strong collider approximation in which it is assumed that single-collision deactivation applies, and (2) on the comparison of such rates with those derived from statistical models (RRKM theory).[7-9]

In this study, the isomerization of CH_3NC by overtone excitation is revisited, but with an emphasis on the role of collisional deactivation. Chandler and Miller[10] have modeled the overtone-induced dissociation of *tert*-butyl hydroperoxide (*t*-BuOOH) via a master equation, and have shown that the product yield resulting from overtone excitation is sensitive to the energy-transfer parameters used in the master equation. The yield was found to vary significantly with the average energy transferred in a deactivating collision. Their best fit to the data of Chandler, Farneth, and Zare,[11] for overtone excited *t*-BuOOH collisions with room temperature *t*-BuOOH, implied an average energy transfer per collision of about -1700 cm^{-1}. More recently, Baggott[12] has used a master equation formalism to analyze his data on the overtone-induced isomerization of cyclobutene and has extracted similar parameters. From his studies, as well as those presented here, it is clear that product yield following overtone excitation is a sensitive function of the details of the collisional deactivation process, even when the molecule is excited just above the reaction barrier and would be expected to be in a "strong collider" regime.

The product yield, which is the observable in these studies, results from the competition between three rates: (1) the specific rate of reaction, $k(E)$, averaged over the distribution of internal energies, denoted by k_u; (2) the rate of collisional deactivation, k_d; and (3) the rate of photoactivation, k_a.

In this study, we assume that the RRKM model adequately describes the dynamics of the overtone excited CH_3NC and use it to calculate $k(E)$. The rate of photoactivation, k_a, is determined from the experimental condition (laser power, absorption cross section, path length etc.). Having both $k(E)$ and k_a, we further assume a single exponential down model for the shape of the energy-transfer function. This means that the probability of a

† Present address: Department of Chemistry, Bowling Green State University, Bowling Green, OH 43403.

(1) Troe, J. *J. Chem. Phys.* **1977**, *66*, 4758.
(2) Rossi, M. J.; Pladziewicz, J. R.; Barker, J. R. *J. Chem. Phys.* **1983**, *78*, 6695.
(3) Hippler, H.; Troe, J.; Wendelken, H. J. *J. Chem. Phys.* **1978**, *78*, 6709.
(4) Tardy, D. C.; Rabinovitch, B. S. *Chem. Rev.* **1977**, *77*, 369.
(5) Reddy, K. V.; Berry, M. J. *Chem. Phys. Lett.* **1977**, *52*, 111.
(6) Reddy, K. V.; Berry, M. J. *Faraday Discuss. Chem. Soc.* **1979**, *67*, 188.
(7) Kassel, L. S. *The Kinetics of Homogeneous Gas Reactions*; Chemical Catalog Co.; New York, 1932.
(8) Marcus, R. A.; Rice, O. K. *J. Phys. Colloid Chem.* **1951**, *55*, 894.
(9) Marcus, R. A. *J. Chem. Phys.* **1952**, *20*, 359. Wieder, G. M.; Marcus, R. A. *J. Chem. Phys.* **1962**, *37*, 1835. Marcus, R. A. *J. Chem. Phys.* **1965**, *43*, 2658.
(10) Chandler, D. W.; Miller, J. A. *J. Chem. Phys.* **1984**, *81*, 455.
(11) Chandler, D. W.; Farneth, W. E.; Zare, R. N. *J. Chem. Phys.* **1982**, *77*, 4447.
(12) Baggott, J. E. *Chem. Phys. Lett.* **1985**, *119*, 47.

0022-3654/86/2090-3544$01.50/0

molecule with an internal energy E having a collision that leaves it with internal energy E' is exponentially dependent upon the energy difference $E - E'$ for E' less than E. The appropriateness of this model will be discussed later. By adjusting the steepness of the exponential of $-\langle\Delta E\rangle_{down}$ in order to fit the experimental data while simultaneously satisfying detailed balance and normalization, we can determine the average energy transferred in a deactivating collision, $-\langle\Delta E\rangle$.

Presented here is a study of the isomerization of methyl isocyanide photoactivated by pumping the 5–0 and 6–0 C–H stretch transitions at 726 nm and 621 nm, respectively, when the sample is placed inside the cavity of a CW dye laser. The threshold energy for this reaction is estimated to be 37.85 kcal/mol[13] so that the fourth C–H stretch overtone ($5\nu_{C-H}$) exceeds the isomerization threshold *only* by about 1 kcal/mol while the fifth ($6\nu_{C-H}$) exceeds this barrier by about 8 kcal/mol. Measurements of the isomerization rate, as determined by gas chromatographic analysis, are carried out for pure methyl isocyanide (5–130 Torr) and for methyl isocyanide diluted in cyclopropane, sulfur hexafluoride, and argon in the ratio 1:25 over the pressure range 10–200 Torr. The reciprocal of the rate of appearance of the CH_3CN product is plotted against pressure (Stern–Volmer analysis). At low pressures such plots deviate from linearity while at higher pressures (greater than 20 Torr) straight-line behavior is observed.

Curvature at low pressure is expected for excitation to both $5\nu_{C-H}$ and $6\nu_{C-H}$ with the distinction that for excitation to $5\nu_{C-H}$, the curvature should be negative (decreasing slope with increasing pressure), and for excitation to $6\nu_{C-H}$, the curvature should be positive (increasing slope with increasing pressure). The curvature is due to the pressure dependence of the averaged isomerization rate, $\overline{k(E)}$. Here, $\overline{k(E)}$ represents $k(E)$ averaged over the energy distribution of the photoactivated molecules. This point will be discussed later and is examined in detail in another communication.[14] The curvature of the overtone data typically is not observed, due to the pressure regime at which it would be present (less than 20 Torr), but its presence ensures that a simple Stern–Volmer analysis, assuming linear plots, will fail. Our data are consistent with those of Reddy and Berry[5,6] for pure CH_3NC. For CH_3NC diluted in a quencher gas (1:25), the errors associated with measuring yields at total pressures lower than $\sim$10 Torr preclude accurate determination of the curvature. Nevertheless, the slope of the linear, high-pressure regime is sensitive to the energy-transfer parameters and is used to determine the average energy transfer per collision.

Having determined the average energy transferred in a deactivating collision from the master equation, we compare our $-\langle\Delta E\rangle$ values to those derived from the model of Troe.[15] Troe has derived an expression relating the bulk collision efficiency, γ_s, to $-\langle\Delta E\rangle$. We find, as did Baggott,[12] that this approximate method is not completely reliable.

Experimental Section

Methyl isocyanide is prepared by the method outlined by Ugi and Meyer.[16] The vapor of this liquid is photolyzed for timed durations, 3–5 min for the fourth overtone and 20–30 min for the fifth, in a Pyrex intracavity photolysis cell outfitted with two quartz windows set at Brewster's angle. The cell dimensions are 0.83 cm i.d. × 25 cm long. All photolyses are carried out at room temperature. The photolysis laser is a home-built dye laser running with LD700 dye pumped by a krypton ion laser for $5\nu_{C-H}$, and with rhodamine 6G pumped by an argon ion laser for $6\nu_{C-H}$. The krypton ion laser setup is much more stable allowing for smaller error bars on those data sets. The setting of the laser wavelength from day to day is reproducible to about ± 2 cm^{-1}. This should be compared to the laser bandwidth, which is about 2 cm^{-1}.

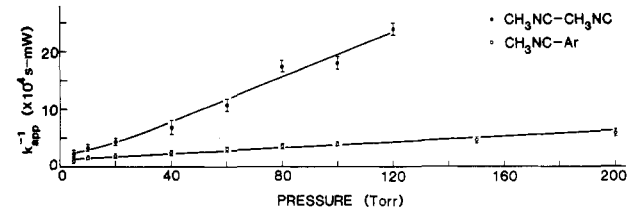

Figure 1. Experimental Stern–Volmer plot for excitation of the CH_3NC $5\nu_{C-H}$ overtone stretching mode.

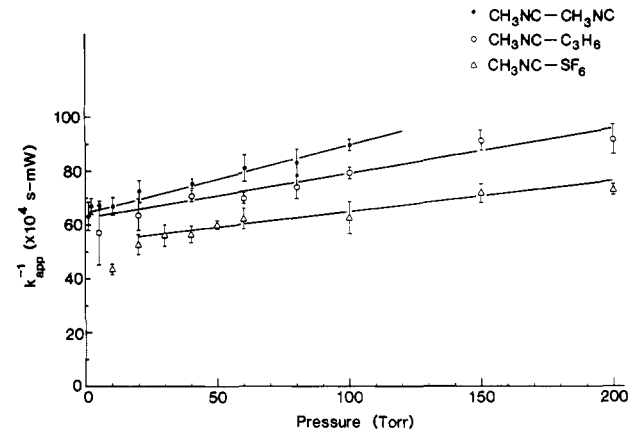

Figure 2. Experimental Stern–Volmer plots for excitation of the CH_3NC $6\nu_{C-H}$ overtone stretching mode.

During photolysis, the laser output power is monitored to ensure intracavity power stability.

After photolysis, the contents of the cell are expanded onto a gas sampling loop and analyzed with a Chromosorb 104 (80/100 mesh) packed column in a Hewlett-Packard 5890A gas chromatograph (GC) with a flame ionization detector. Due to the nonlinearity in the detection of the relative amounts of CH_3NC to CH_3CN as the total pressure of the gas analyzed varied, calibration curves for 2% and 5% mixtures of CH_3CN in CH_3NC are determined. All the data presented have been corrected for this problem. Separate calibration curves for pure CH_3NC and the C_3H_6, SF_6, and Ar dilutions are necessary. All photolyses are run to between 2% and 5% completion in order to keep within these known limits. The nonlinearity in the calibration curves arises from the surface adsorption of CH_3NC. The dilutions are made by expanding 4 Torr of CH_3NC into a glass bulb and then filling with bath gases to a total pressure of 200 Torr for a final 1:25 dilution. This dilution is high enough to ensure that the collisions are predominately between Ar–CH_3NC, but low enough to make dependable GC analyses. For the $6\nu_{C-H}$ data, a Datametrics Model 1174 Barocel electronic manometer and a Wallace Tiernan Model FA160 pressure gauge are used. The $5\nu_{C-H}$ data are obtained by using a Wallace Tiernan Series 66-200 digital pressure gauge.

Results

Figures 1 and 2 present Stern–Volmer plots for excitation of the $5\nu_{C-H}$ and $6\nu_{C-H}$ overtones of CH_3NC. These plots give k_{app}^{-1} in convenient experimental units, [fraction of CH_3NC produced/(s)(mW output power)]$^{-1}$. It is observed that in both figures the slope of the CH_3NC–M dilution data is less than that of the CH_3NC–CH_3NC data, indicating that C_3H_6, SF_6, and Ar are less efficient collider gases than CH_3NC itself. There is curvature present in both plots at low pressure. These deviations from linearity are outside of our experimental error; therefore, we limit our analysis to the high-pressure linear region.

Table I gives the slopes and extrapolated high-pressure intercepts computed from least-squares fits to the data. It can be seen that the intercepts for the CH_3NC–CH_3NC and CH_3NC–M data are not the same. This is to be expected since different collider partners will exhibit differing amounts of low-pressure curvature. Extrapolation of high-pressure data will therefore lead to erroneous intercepts. The slope of the CH_3NC–Ar data is about 11% of

(13) Maloney, K. M.; Rabinovitch, B. S. In *Isonitrile Chemistry*, Ugi, I., Ed.; Academic: New York, 1971; p 41.
(14) Miller, J. A.; Chandler, D. W.; accepted for publication in *J. Chem. Phys.*
(15) Troe, J. *J. Phys. Chem.* **1983**, *87*, 1800; *J. Chem. Phys.* **1977**, *66*, 4745.
(16) Ugi, I.; Meyer, R. *Chem. Ber.* **1960**, *93*, 239.

TABLE I: Slopes and Intercepts of Stern-Volmer Plots

overtone transition	collider gas	slope	intercept
5–0	CH_3NC^a	$1.80 \times 10^3 \pm 0.06 \times 10^3$	$1.0 \times 10^4 \pm 0.4 \times 10^4$
	Ar^b	$0.20 \times 10^3 \pm 0.02 \times 10^3$	$2.0 \times 10^4 \pm 0.2 \times 10^4$
6–0	CH_3NC^a	$2.30 \times 10^3 \pm 0.20 \times 10^3$	$66.2 \times 10^4 \pm 0.9 \times 10^4$
	$C_3H_6^c$	$1.50 \times 10^3 \pm 0.20 \times 10^3$	$64.0 \pm 10^4 \pm 2.0 \times 10^4$
	SF_6^c	$0.90 \times 10^3 \pm 0.10 \times 10^3$	$56.0 \times 10^4 \pm 1.0 \times 10^4$
	Ar^d	$0.30 \times 10^3 \pm 0.10 \times 10^3$	$60.0 \times 10^4 \pm 1.0 \times 10^3$

[a] All data points are used since the curvature is not pronounced. [b] Data points for 5, 10, and 20 Torr are omitted. [c] Data points for 10 and 20 Torr are omitted. [d] Larger error bars are due to insensitivity of yield to weak colliders at these energies.

that found for the CH_3NC–CH_3NC data for the fourth overtone. The slopes of the CH_3NC–C_3H_6 and CH_3NC–SF_6 data are about 65% and 40%, respectively, of that found for the CH_3NC–CH_3NC data for the fifth overtone.

Data for a 1:25 dilution of CH_3NC–Ar are also collected for excitation into the fifth overtone. The slope for this dilution is around 13% of that found for the pure gas. However, this data has larger errors, due to our lack of sensitivity to small changes in the yield (collisions do not strongly inhibit isomerization).

Discussion

The change in the slope and intercept for the Stern–Volmer lines for pure CH_3NC–CH_3NC vs. CH_3NC–M must be due to collisional effects. In thermal activation studies,[17] C_3H_6, SF_6, and Ar have been shown to be less efficient in collisional energy transfer with CH_3NC than CH_3NC colliding with itself. In order to understand this weak collision effect, the Stern–Volmer model is reexamined. In the standard Stern–Volmer treatment, one assumes a photoactivation step

$$CH_3NC + h\nu \xrightarrow{k_a} CH_3NC^* \quad (1)$$

characterized by the rate k_a, an isomerization step

$$CH_3NC^* \xrightarrow{k_u} CH_3CN \quad (2)$$

characterized by the specific unimolecular rate constant k_u which competes with collisional deactivation

$$CH_3NC^* + M \xrightarrow{k_d} CH_3NC + M \quad (3)$$

In this model the inverse of the rate coefficient for the appearance of the CH_3CN product is given by

$$\frac{1}{k_{app}} = \frac{1}{k_a[h\nu]} + \frac{k_d[M]}{k_u k_a[h\nu]} \quad (4)$$

where $[h\nu]$ is the photon density. Hence when k_{app}^{-1} is plotted against [M], a straight line is obtained with an intercept $1/(k_a[h\nu])$ and a slope $k_d/(k_u k_a[h\nu])$.

Deactivation Rate Constant k_d. In the standard Stern–Volmer analysis used for overtone excitation data, k_d is commonly taken to be the collisional frequency, Z. An important conclusion of this study, as well as ref 14, is that for CH_3NC collisions with CH_3NC, k_d is not equal to Z, even very near the threshold. When working in a single-collision deactivation regime, we should rewrite k_d as the product of two factors

$$k_d = \gamma Z \quad (5)$$

where γ is a collision efficiency factor and Z is the collision frequency. The value of γ must be determined by experiment and expresses the change in the deactivation rate that is not accounted for by the change in collision frequency, Z. Clearly, the value of γ will depend on which collision frequency is chosen to represent the collision process, e.g., hard sphere, Lennard-Jones (12–6), Stockmayer (12–6–3), etc. The relative ordering of γ values for many different collider gases studied by using thermal, chemical, and photochemical activation is the same. Attempts have been made to find a correlation for this relative ordering with many molecular properties, such as polarizability, dipole moment, boiling point, number of atoms in the collider gas, and relative molecular complexity, but no one scheme seems totally satisfactory.[17,18]

TABLE II: Collision Number and Collision Parameters Using the Stockmayer Potential

collision partners	σ_M, Å	ϵ_M/k, K	$\Omega_{AM}^{(2,2)*}$	Z_s, Torr/s
CH_3NC–CH_3NC	4.47	380	1.75	1.99×10^7
CH_3NC–SF_6	4.74	259	1.23	1.25×10^7
CH_3NC–C_3H_6	4.57	303	1.28	1.50×10^7
CH_3NC–Ar	3.42	124	1.09	9.58×10^6

For thermal activation studies, collision frequencies are usually calculated from Lennard-Jones collision parameters for nonpolar molecules and from the Stockmayer collision parameters for polar molecules.[18] The Stockmayer collision parameters[17] used in this work are given in Table II along with the collision frequencies calculated according to Troe.[1] For CH_3NC–CH_3NC, the Stockmayer collision frequency, Z_s, is 1.99×10^7 Torr/s. For CH_3NC–C_3H_6, CH_3NC–SF_6, and CH_3NC–Ar, the collision frequencies are 1.50×10^7, 1.25×10^7, and 9.58×10^6 Torr/s, respectively.

It is interesting to note that Z_{HS} calculated according to the hard-sphere model[19] using a diameter of 4.97[6] and 2.86 Å[19] for CH_3NC and Ar, respectively, give values which are factors of 1.4 and 2.1 larger than Z_s. For this work, we have chosen to use the Stockmayer collision frequencies. This choice is the normal one for polar collision partners. We denote the corresponding collision efficiency factor by γ_s.

Master Equation Model. The photoactivated unimolecular isomerization of CH_3NC can be described by the integral form of the time-dependent master equation

$$\frac{dy(E,t)}{d(Zt)} = \int_0^\infty y(E',t)\, p(E',E)\, dE' - y(E,t)\int_0^\infty p(E,E')\, dE' - k(E)\, y(E,t)/Z$$

$$\frac{dy_p(t)}{d(Zt)} = \int_0^\infty k(E)\, y(E,t)\, dE/Z \quad (6)$$

In eq 6, $y(E',t)\, dE'$ is the probability of finding a molecule in a state between energy E' and $E' + dE'$ at a time t, $p(E,E')\, dE'$ is the probability per collision of a molecule of energy E being transferred with energy between E' and $E' + dE'$, $k(E)$ is the unimolecular isomerization rate constant for a molecule with internal energy E, Z is the collision frequency (discussed above, and listed in Table II), and $y_p(t)$ is the probability of finding product at time t. The total yield is $y_p(\infty)$. The product Zt is a dimensionless quantity interpreted as the average number of collisions suffered by a molecule up to time t.

In order to solve eq 6 for the time history of $y(E,t)$, and therefore $y_p(t)$, we need to supply an initial distribution, taken to be the thermal distribution displaced by the photon energy, a model for unimolecular isomerization, RRKM theory, and a model for collisional deactivation, taken to be exponential down

$$P_{down}(E,E') = \exp(-|\Delta E|/\Gamma), \quad E > E' \quad (7)$$

Any energy-transfer probability density function must simulta-

(17) Chan, S. C.; Rabinovitch, B. S.; Bryant, J. T.; Spicer, L. D.; Fujimoto, T.; Lin, Y. N.; Pavlov, S. P. *J. Phys. Chem.* **1970**, *74*, 3160.

(18) Quack, M.; Troe, J. *Gas Kinetics and Energy Transfer*; Ashmore, P. G.; Donovan, R. J., Eds.; The Chemical Society: London, 1977; Vol. 2, p 175.

(19) Moore, W. J. *Physical Chemistry*, 4th ed.; Prentice-Hall: Englewood Cliffs, NJ, 1972; p 149.

neously satisfy two criteria, normalization (conservation of mass) and detailed balance. These can be written

$$\int_0^\infty P(E,E')\,dE' = 1 \tag{8}$$

and

$$P(E,E')y_{eq}(E) = P(E',E)\,y_{eq}(E') \tag{9}$$

where $y_{eq}(E)$ is the equilibrium population distribution. Equations 7, 8, and 9 completely define a probability density function.

A simple exponential down probability density function has the advantage of being able to make the connection that Γ is equal to the average energy transferred in a deactivating collision, $-\langle\Delta E\rangle_{down}$. Further, Procaccia and Levine[20] have shown, from an information theoretical approach, that under the constraint of knowing only the first moment of the distribution, an exponential function maximizes the information entropy and is therefore the most natural choice. Our knowledge of the energy-transfer function is limited to the first moment, at most. Tardy and Rabinovitch[21] suggest that for a "strong collider" a Gaussian energy-transfer shape should be more appropriate than an exponential shape. In ref 14 the effect of different function shapes (exponential, Gaussian, Poisson, and double exponential) is investigated for the case of overtone excited methyl isocyanide. It is found that the value of $-\langle\Delta E\rangle_{down}$ consistent with the data of Reddy and Berry is 20% lower for a Gaussian shape than for an exponential shape; this difference is well within the combined uncertainties of the data and calculation. We conclude that the changes in the function shape could have a small effect on the absolute value of $-\langle\Delta E\rangle_{down}$ extracted from the data but not the trends observed here. Details of the calculation and the sensitivity of the yield to different probability density function shapes are discussed in greater detail in ref 14.

The unimolecular isomerization rates, $k(E)$, were calculated by using RRKM theory. Initially, the "300 model" parameters[13] were used in the calculation. The 300 model is the best guess parameters fitted to thermal isomerization data[13] and were the RRKM parameters used by Reddy and Berry.[6] We found, however, that it was not possible to match the lower overtone data of Reddy and Berry for any collision efficiency using the 300 model parameters. The 300 model produces more product, by a factor of 2 more than they observed, even if the average energy transferred down per collision is assumed to be infinite. Additionally, the 300 model gave $-\langle\Delta E\rangle_{down} = 4000$ cm^{-1} as the best fit to Reddy and Berry's upper overtone data set for CH_3NC colliding with itself. This value is unreasonably high. The failure of the 300 model to describe overtone isomerization data is sufficiently serious to require a reexamination of the assumptions inherent in the master equation analysis. These include single-exponential down transfer probability function, 300 model parameters, harmonic oscillator approximation in the calculation of $k(E)$, and the appropriateness of using RRKM theory on a molecule as small as CH_3NC. All of these alternatives, including some combinations, are possible. Maloney and Rabinovitch[13] report the effect of neglecting anharmonicity in calculating $k(E)$ for methyl isocyanide and report that this introduces a 15% change, insufficient to explain the observed descrepancy of a factor of 2.

One possibility is a change in the 300 model isomerization barrier height. We found that an increase in the isomerization barrier by 200 cm^{-1} gave a best fit for both the upper and lower overtone data sets with the same value of $-\langle\Delta E\rangle_{down}$; namely, $-\langle\Delta E\rangle_{down} = 1200$ cm^{-1}. Additionally, use of this higher barrier accurately fit the curvature observed by Reddy and Berry for excitation at $6\nu_{C-H}$. This "threshold modified 300 model" was used in all subsequent calculations. The ability of this modified parameter set to fit the CH_3NC–CH_3NC data gave us confidence that the isomerization process could be adequately described by RRKM theory using a single-exponential down model. We do not mean to imply that the barrier height is necessarily wrong in the 300 model, only that it is one reasonable possibility.

In order to fit the data, the yield, $y_p(\infty)$, as a function of pressure, was calculated for different values of Γ for each data set. Typical calculated data sets are shown in Figures 3 and 4. Figures 3 and 4 show data for collisions of Ar with CH_3NC after excitation at $5\nu_{C-H}$ and $6\nu_{C-H}$, respectively. By variation of Γ in order to fit the high-pressure linear portions of the experimental data sets (Figures 1 and 2), the average energy transferred in a down collision, $-\langle\Delta E\rangle_{down}$, as well as the average energy transferred per collision, $-\langle\Delta E\rangle$, were determined for each collision partner. These are listed in Table III.

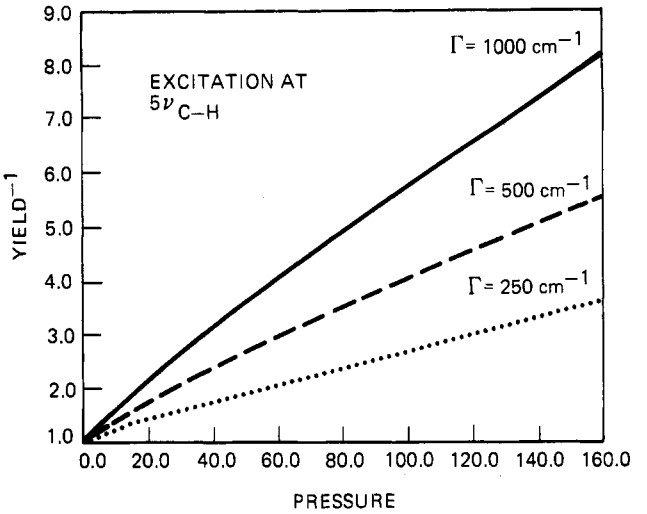

Figure 3. Calculated Stern–Volmer plots for CH_3NC–Ar mixtures after excitation of the CH_3NC $5\nu_{C-H}$ overtone stretching mode. Γ is the average energy transferred in a deactivating collision.

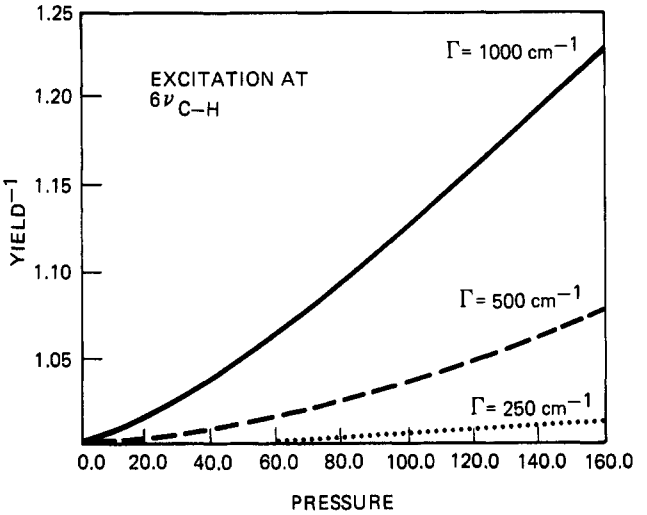

Figure 4. Calculated Stern–Volmer plots for CH_3NC–Ar mixtures after excitation of the CH_3NC $6\nu_{C-H}$ overtone stretching mode. Γ is the average energy transferred in a deactivating collision.

TABLE III: Collisional Energy-Transfer Parameters As Determined by Master Equation Analysis

	press. range of fit, Torr	$-\langle\Delta E\rangle_{down}$, cm^{-1}	$-\langle\Delta E\rangle$, cm^{-1}
	5–0 Overtone		
CH_3NC	40–100	1375	1172
Ar	60–160	375	228
	6–0 Overtone		
CH_3NC	60–100	1375	1172
Ar			
C_3H_6	60–100	1000	807
SF_6	60–140	1100	904

(20) Procaccia, I.; Levine, R. D. *Chem. Phys. Lett.* **1975**, *33*, 5; *J. Chem. Phys.* **1975**, *62*, 2496.
(21) Tardy, D. C.; Rabinovitch, B. S. *J. Chem. Phys.* **1968**, *48*, 1282.

Our value of $-\langle\Delta E\rangle = 1172$ cm^{-1} for CH_3NC is smaller than that found from the thermal experiments, but the values for SF_6 ($-\langle\Delta E\rangle = 904$ cm^{-1}) and Ar ($-\langle\Delta E\rangle = 228$ cm^{-1}) are comparable. It should be noted that these quantities are average energy transferred per collision, not energy transferred down, which is typically the quantity reported from thermal studies.[17]

The $-\langle\Delta E\rangle$ values extracted for CH_3NC^* with SF_6 (904 cm^{-1}) and Ar (228 cm^{-1}) can be compared to the lower values of $-\langle\Delta E\rangle$ found for overtone excited cyclobutene[12] with SF_6 (323 cm^{-1}) and Ar (35 cm^{-1}). Part of these differences can be attributed to the different molecular systems involved, but probably not all. It is important to recall that the cyclobutene was excited at 16603 cm^{-1}, well above threshold (11 319 cm^{-1}). It might be expected that the yields would not be as sensitive to the energy-transfer parameters under these conditions as when the excitation is nearer threshold.

Other values of $-\langle\Delta E\rangle$ for Ar and SF_6 with large polyatomics have been deduced by the technique of time-resolved infrared emission following excitation by Barker and co-workers.[2] He obtains values of $-\langle\Delta E\rangle$ of 119 cm^{-1} for Ar and 351 cm^{-1} for SF_6, in collisions with hot azulene. Troe[3] has determined these parameters for collision with hot toluene. His determination of $-\langle\Delta E\rangle$ for Ar and SF_6 were 130 and 400 cm^{-1}, respectively. Our values of $-\langle\Delta E\rangle$ for Ar and SF_6 may not be a significant difference, considering the difference in molecular systems. No consistent picture has yet to emerge from these various studies. Clearly, further studies are needed to explain satisfactorily the values of $-\langle\Delta E\rangle$ and how they may vary with the degree of excitation and collision partner.

Examination of Figures 3 and 4 shows that curvature is expected in these Stern–Volmer plots. The curvature can be traced to the pressure dependence of the dissociation rate constant, k_u, which can be explained in terms of the pressure dependence of the reactive distribution. This is discussed in the next section.

Specific Rate Constant, $k(E)$. The photoactivation process in our experiment creates a distribution of total energies in the activated molecules. The local-mode approximation to overtone excitation dictates that this initial distribution is simply the room temperature Boltzmann distribution displaced by the energy of the photon, although exceptions are known.[22] If this distribution is formed high enough above the reaction barrier (excitation at $6\nu_{C-H}$), single-collision events will not cause complete deactivation. As inelastic collisions occur, the mean energy and shape of this distribution shifts, causing curvature in the Stern–Volmer plot. At still higher pressures, the Stern–Volmer plot appears linear.

It may seem paradoxical that the simple Stern–Volmer model fails while at the same time the Stern–Volmer plots appear linear at high pressure. The reason for the linear behavior at high pressure can be traced to the shape of the time-averaged distribution of photoactivated molecules that becomes pressure-independent as the collision rate exceeds the reaction rate. The slope of the Stern–Volmer plot reflects the convolution of this constant distribution with the $k(E)$ curve. As a result, the measured rate will be dependent on both the pressure and the collider gas present.

This behavior was studied by Kohlmaier and Rabinovitch[23] for chemically activated *sec*-butyl radicals in helium, neon, argon, and krypton. In these experiments, the effect of strong and weak colliders on the observed rate constant was studied and discussed in term of the energy distribution in the molecules. Likewise, the specific rate constant measured by overtone pumping (the k_u in eq 4) is an average rate[11] and hence is denoted by $\overline{k(E)}$, the average measured specific rate constant.

If the initial distribution is formed close to the reaction barrier (excitation at $5\nu_{C-H}$), where $k(E)$ is strongly varying over the distribution, then the lower energy wing of the distribution will be preferentially deactivated relative to the upper energy wing of the distribution, which reacts more rapidly. In this case, increasing the pressure increases the observed rate constant since only the high-energy wing of the distribution reacts. Once again, the shape of the distribution becomes constant with increasing pressure leading to a linear Stern–Volmer plot. This effect was noted in the overtone dissociation of *t*-BuOOH[10,11] and is discussed in detail as it pertains to CH_3NC in ref 14.

TABLE IV: Collisional Energy-Transfer Parameters, $-\langle\Delta E\rangle$, Determined by Eq 10 and 11 Using "300 Model" RRKM Parameters

transition	gas	γ_s	$-\langle\Delta E\rangle$, kcal/mol	$-\langle\Delta E\rangle$, cm^{-1}
5–0	CH_3NC	1.80 ± 0.08		
	Ar	0.21 ± 0.01	0.26	93
6–0	CH_3NC	0.71 ± 0.06	3.90	1400
	C_3H_6	0.64 ± 0.05	3.00	1100
	SF_6	0.51 ± 0.08	2.90	1000

Approximate Method. Troe[15] has derived, using approximations to a master equation, a formula relating γ_s to $-\langle\Delta E\rangle$. Baggott,[12] in his recent study of overtone-induced isomerization of cyclobutene, found that this model underestimated $-\langle\Delta E\rangle$ by at least a factor of 2, even with strong colliders, where the model should be best. We, too, use Troe's model to estimate $-\langle\Delta E\rangle$ and compare to our values obtained from solution of the master equation using the appropriate RRKM parameters.

By fitting the high-pressure data to a straight line and substituting eq 5 into eq 4, we can deduce the relative collision efficiencies for the different collider gases for a given $k(E)$. The original 300 model was used to extract γ_s from the data of Table I for the case of CH_3NC–CH_3NC collisions.

Once the collision efficiency γ_s is obtained, the average amount of energy transferred per collision, $-\langle\Delta E\rangle$, can be estimated by using the approximate relation[15]

$$\frac{\gamma_s}{1-\gamma_s^2} = \frac{-\langle\Delta E\rangle_s^{**}}{(E-E_0+C)\left[1-\left(\frac{C}{E-E_0+C}\right)^s\right]} \quad (10)$$

Here, s^{**} describes the energy dependence of the specific rate constant which is assumed to have the functional form

$$k(E) \propto (E-E_0+C)^{s^{**}-1} \quad (11)$$

where C is a constant. We use in eq 10 $s^{**} = 7.98$ and $C = 14.64$ based on fitting the $k(E)$ values of Reddy and Berry[6] to eq 11. For E, we take the value of $h\nu$ corresponding to the overtone transition and for E_0 the threshold energy (37.85 kcal/mol). The results of this analysis are presented in Table IV.

For excitation to $5\nu_{CH}$, the best fit to the data gives a γ_s exceeding unity ($\gamma_s = 1.8$). This value of γ_s for CH_3NC collisions with overtone excited CH_3NC is consistent with the master equation solution which found that no value of Γ in eq 9 could fit the data with the 300 model. For the upper overtone, $6\nu_{C-H}$, the approximate method using the 300 model yielded a value of $-\langle\Delta E\rangle$ of 1400 cm^{-1} which is fortuitously close to the answer obtained by solution of the master equation using the "threshold modified 300 model". The value of $-\langle\Delta E\rangle$ of 1400 cm^{-1} must be compared to the $-\langle\Delta E\rangle$ obtained by using the 300 model in the master equation. With the 300 model, the master equation yielded a $-\langle\Delta E\rangle$ of 3800 cm^{-1}; therefore, eq 10 underestimates the $-\langle\Delta E\rangle$ obtained by solution of the master equation for the same RRKM parameters and data. We suspect that this failure may arise because eq 10 is not valid for large γ_s.

Concluding Remarks. All the overtone isomerization data for CH_3NC to CH_3CN were modeled satisfactorily by using the RRKM framework to describe the reaction rate as a function of energy, and using a single-exponential down transfer probability function to describe the collision dynamics. Solution of the master equation yielded the average energy transferred per collision for various collider partners with CH_3NC. We found that $-\langle\Delta E\rangle$ decreases in the order CH_3NC, C_3H_6, SF_6, Ar. Moreover, the $-\langle\Delta E\rangle$ values obtained are intermediate between those derived from thermal activation studies and those derived from "direct studies". The present technique is applicable to a large number

(22) Chuang, M.-C.; Zare, R. N. *J. Chem. Phys.* **1985**, *82*, 3714.
(23) Kohlmaier, G. H.; Rabinovitch, B. S. *J. Chem. Phys.* **1963**, *38*, 1692.

of molecular systems and should yield energy-transfer parameters with a comparable level of confidence to those reported by other methods.

Acknowledgment. This research was supported by Standard Oil Co. (Indiana) (D.L.S. and R.N.Z.) and by the U.S. Department of Energy, Office of Basic Energy Sciences, Division of Chemical Sciences (J.A.M. and D.W.C.).

Registry No. Methyl isocyanide, 593-75-9.

Infrared Multiphoton Dissociation of Three Nitroalkanes

A. M. Wodtke, E. J. Hintsa, and Y. T. Lee*

Materials and Molecular Research Division, Lawrence Berkeley Laboratory, and Department of Chemistry, University of California, Berkeley, California 94720 *(Received: January 28, 1986; In Final Form: March 12, 1986)*

Infrared multiphoton dissociation in a molecular beam has been studied in order to elucidate the collision-free "thermal" chemistry and dynamics of nitromethane, nitroethane, and 2-nitropropane. The isomerization of CH_3NO_2 to CH_3ONO was observed by detecting the CH_3O and NO products from the dissociation of the internally very hot, isomerized nitromethane. A novel application of RRKM theory was used to estimate the barrier height to isomerization at 55.5 kcal/mol. The barrier height determination method was tested and found to give excellent results by applying it to the determination of the barrier height to HONO elimination from nitroethane, a value which is well-known from activation energy measurements. The method was then applied to the case of HONO elimination from 2-nitropropane and it appears that there is good reason to believe that the barrier height is 3–5 kcal/mol lower in 2-nitropropane than in nitroethane. The success of this method for determining barrier heights shows how a "microscopic" molecular beam experiment, using infrared multiphoton dissociation where the concept of temperature has no place, can be quantitatively related to pyrolysis experiments which are conducted under collisional, thermal conditions and measure phenomenological quantities such as activation energies. The concerted HONO elimination reactions from nitroethane and 2-nitropropane were found to channel about 70 and 65% of the exit barrier into translation, respectively. This large release of translational energy is suggested to be due to the nature of the transition-state mechanical barrier which is largely made up of repulsive energy between the closed shell products and not of reactant strain energy. The small difference between nitroethane and 2-nitropropane in the translational energy distributions is explained in terms of a scaled reduced mass impulse approximation that is used to characterize the repulsive excitation dynamics of the departing closed shell products.

I. Introduction

The discovery of infrared, multiple-photon absorption (IRMPA) and dissociation (IRMPD) in isolated polyatomic molecules raised great hopes that one could direct chemical reactions, since IRMPA allows one to put a great deal of energy directly into the nuclear motion of a polyatomic molecule through a specific vibrational degree of freedom.[1-5] The subsequent discovery that IRMPD could be isotopically selective[6-8] aroused continued enthusiasm among some scientists about the possibilities of bond selective chemistry. A plethora of review articles has appeared on these and related topics.[9] It is now generally realized that the quest for mode-specific chemistry by IRMPD is not technologically possible because of very fast intramolecular vibrational redistribution (IVR) in highly vibrationally excited polyatomic molecules. Several experiments have shown that this typically occurs on a picosecond time scale or faster.[10,11] The profound implications of this can be appreciated if one realizes that even for strong IR absorbers ($\sigma = 10^{-17}$ cm^2) and intense IR sources ($I = 10^{26}$ photons cm^{-2} s^{-1}), the average time it takes to absorb a *single* photon is 10^{-9} s.

In spite of the "problem" of picosecond IVR, in fact because of it, there are certain advantages to studying the dissociation of polyatomic molecules by IRMPD. The first of these is that statistical theories of unimolecular decomposition[12] which assume the free flow of vibrational energy in the dissociating molecule can be used to describe the dissociation process and thus interpret experimental results. The validity and usefulness of various statistical theories, especially the most commonly used RRKM theory, have been widely documented in the literature.[13-18]

(1) Isenor, N. R.; Richardson, M. C. *Appl. Phys. Lett.* **1971**, *18*, 224.
(2) Isenor, N. R.; Richardson, M. C. *Opt. Commun.* **1971**, *3*, 360.
(3) Letokhov, V. S.; Ryabov, E. A.; Tumanov, O. A. *Opt. Commun.* **1972**, *5*, 168.
(4) Letokhov, V. S.; Ryabov, E. A.; Tumanov, O. A. *Sov. Phys.-JETP (Engl. Transl.)* **1973**, *36*, 1069.
(5) Isenor, N. R.; Merchant, V.; Halworth, R. S.; Richardson, M. C. *Can. J. Phys.* **1973**, *51*, 1281.
(6) Ambartzumian, R. V.; Gorokov, Yu. A.; Letokhov, V. S.; Makarov, G. N. *JETP Lett. (Engl. Transl.)* **1974**, *21*, 171.
(7) Ambartzumian, R. V.; Gorokov, Yu. A.; Letokhov, V. S.; Makarov, G. N. *JETP Lett. (Engl. Transl.)* **1975**, *43*, 22.
(8) Lyman, J. L.; Jensen, R. J. Rink, J.; Robinson, C. P.; Rockwood, S. D. *Appl. Phys. Lett.* **1975**, *27*, 87.
(9) See for example: Bloembergen, N.; Yablonovitch, E. *Phys. Today* **1978**, May, 23–30. Ashfold, M. N. R.; Hancock, G. *Gas Kinet. Energy Transfer* **1980**, *4*, 73–116. Cantrell, C. D.; Freund, S. M.; Lyman, J. L. *The Laser Handbook*; Stitch, M. L., Ed.; North Holland: Amsterdam, 1979; pp 485–576. Schultz, P. A.; Sudbo, Aa. S.; Krajnovich, D. J.; Kwok, H. S.; Shen, Y. R.; Lee, Y. T. *Annu. Rev. Phys. Chem.* **1979**, *30*, 379.
(10) Rynbrandt, J. D.; Rabinovitch, B. S. *J. Phys. Chem.* **1971**, *75*, 2164.
(11) Maier, J. P.; Seilmeier, A.; Laubereau, A.; Kaiser, W. *Chem. Phys. Lett.* **1977**, *46*, 527.
(12) Robinson, P. J.; Holbrook, K. A. *Unimolecular Reactions*: Wiley: London, 1972.
(13) Coggiola, M. J.; Schultz, P. A.; Lee, Y. T.; Shen, Y. R. *Phys. Rev. Lett.* **1977**, *38*, 17.
(14) Grant, E. R.; Coggiola, M. J.; Lee, Y. T.; Schultz, P. A.; Sudbo, Aa. S.; Shen, Y. R. *Chem. Phys. Lett.* **1977**, *52*, 595.
(15) Sudbo, Aa. S.; Schultz, P. A.; Grant, E. R.; Shen, Y. R.; Lee, Y. T. *J. Chem. Phys.* **1978**, *68*, 1306.
(16) Sudbo, Aa. S.; Schultz, P. A.; Grant, E. R.; Shen, Y. R.; Lee, Y. T. *J. Chem. Phys.* **1979**, *70*, 912.
(17) Butler, L. J.; Buss, R. J.; Brudzynski, R. J.; Lee, Y. T. *J. Phys. Chem.* **1983**, *87*, 5106.
(18) Huisken, F.; Krajnovich, D.; Zhang, Z.; Shen, Y. R.; Lee, Y. T. *J. Chem. Phys.* **1983**, *78*, 3806.

0022-3654/86/2090-3549$01.50/0